



Numerical Approach to Assess Wax Removal by Heating

Ivan Ibanez A.* , Angela O. Nieckele, Luís Fernando A. Azevedo

Department of Mechanical Engineering, PUC-Rio, Rio de Janeiro, RJ, Brazil, *iibanez@puc-rio.br

Abstract

Wax deposition phenomena in pipelines is one of most critical problems faced by the oil transport industry. Hot oil is extracted from the reservoir, and it is transported by pipelines to the refineries, losing heat to the environment. If the temperature drops below the WAT (wax appearing temperature), paraffin crystals precipitate and they can deposit along the pipeline walls, causing reduction of the oil flow rate or even in some extreme cases, causing total obstruction of the duct. Ideally, one desires to avoid the deposit formation, however, when it is formed, different strategies can be applied to remediate the problem (cleaning with PIG, insulating, adding chemical, and heating the flow). The present study seeks to numerically evaluate the strategy of removing the wax deposit, by heating the duct wall. In order to identify the influence of deposit thickness and aging on the time required to remove the deposit, different heating procedures were examined. The necessary heating rate and removal times for each case were determined. Solid fraction, temperature and velocity fields during the removal process were also analyzed.

Keywords

Wax deposition; Removal by heating; Flow Assurance

Introduction

One of the most relevant problems in production and transportation petroleum pipelines is formation of paraffin deposits. In subsea production system, where the environmental temperature is low, the oil transported loses heat to the cold sea water, and heavier paraffins components may precipitate and solidify in the regions close to the pipeline wall [1]. Wax deposit can generate serious problems such as the reduction of the oil mass flow or total loss of the production line. During the wax deposition process, heat transfer and mass transfer processes play relevant roles, especially in the deposit growth rate and deposit aging stages [2]. Different strategies have been investigated in order to mitigate wax deposits, such as wax removal by PIG [3]; thermal insulation [4]; application of chemical [5]; wax removal by heating [6] and soaking [7].

Bell et al. [6] experimentally observed that for wax deposits with low content of heavy species, it is possible to remove a significant portion of the deposit (63%) with heating temperatures up to 4% lower than the WAT. The cooling period can influence the heat removal performance, because as the cooling period increases, the deposit ages and consequently the removal time can change. Again, in relation to the cooling period, the study performed by Ventura et al. [8] evaluates its influence on the time required for the flow restart after a shutdown stage. They noticed that as the cooling period increased, a larger pressure drop was required for the flow restart take place.

The present study seeks to numerically evaluate, through computational fluid dynamics, the

influence of the cooling period on the efficiency of the technique of wax removal by heating the duct wall.

Mathematical Model

In this study, the mixture model (formed by liquid l and solid s phases) was employed to obtain the conservation equations, as proposed by Fleming [9]. The fluid is formed by several species i , which can be present in both phases. The deposit is the region with solid volume fraction S_s above 2%, as recommended by Holder and Winkler [10].

The equations for conservation of mass, species, momentum, and energy are

$$\frac{\partial}{\partial t}(\rho_m) + \nabla \cdot (\rho_m \mathbf{u}_m) = 0 \quad (1)$$

$$\frac{\partial}{\partial t}(\rho_{m,i}) + \nabla \cdot (\rho_{m,i} \mathbf{u}_m) = -\nabla \cdot \mathbf{j}_i \quad (2)$$

$$\frac{\partial}{\partial t}(\rho_m \mathbf{u}_m) + \nabla \cdot (\rho_m \mathbf{u}_m \mathbf{u}_m) = -\nabla p + \nabla \cdot \boldsymbol{\tau}_m \quad (3)$$

$$\nabla \cdot (\lambda_m \nabla T) = \frac{\partial}{\partial t}(\rho_m h_m) + \nabla \cdot (\rho_m h_m \mathbf{u}_m) + \nabla \cdot \left(\sum_{i=1}^N \mathbf{j}_i h_{i,l} \right) \quad (4)$$

where \mathbf{u}_m , $\rho_{m,i}$ are the mixture velocity and mass fraction of species i . p and T are the pressure and temperature. ρ is density and λ refers to thermal conductivity. \mathbf{j}_i is diffusive flux of each specie i , $h_{i,l}$ is the enthalpy of specie i in the liquid phase and $\boldsymbol{\tau}_m$ is the mixture viscous stress tensor.

Both phases velocities are equal to the mixture velocity \mathbf{u}_m , while the mixture enthalpy h_m is mass based

$$h_m = (S_l \rho_l h_l + S_s \rho_s h_s) / \rho_m \quad ; \quad S_l = 1 - S_s \quad (5)$$

Here, the subscripts m, l and s refer to mixture, liquid and solid phase, respectively. The mixture properties are

$$\rho_m = S_l \rho_l + S_s \rho_s \quad ; \quad \lambda_m = S_l \lambda_l + S_s \lambda_s \quad (6)$$

The diffusive flux of each specie i is

$$\mathbf{j}_i = -D_i \nabla c_{i,l} S_l \rho_l \quad (7)$$

where D_i is the Fick's binary diffusion coefficient between the solvent and each specie i , and it calculated from the Hayduk and Minhas Correlation [11] and $c_{i,l}$ refers to the mass fraction of specie i in the liquid phase, determined through the thermodynamic model of multiple solid solutions [12].

The mixture viscous stress tensor is defined as a Newtonian fluid by

$$\boldsymbol{\tau}_m = \mu_m 2 \mathbf{S} \quad ; \quad \mathbf{S} = \frac{1}{2} (\nabla \mathbf{u}_m + \nabla^T \mathbf{u}_m) \quad (8)$$

$$\mu_m = \mu_l e^{\Omega S_s} \quad (9)$$

where the mixture viscosity μ_m depends on the solid volume fraction, where Ω is a fitting parameter of the model based in rheometric characteristic of the mixture.

The mass fraction of specie i in phase $k = l, s$ ($c_{i,k}$), the solid volume fraction S_s and enthalpy h are also obtained with the thermodynamic model [12].

The liquid and solid density, as well as the liquid viscosity are determined with the model proposed by Queimada et al. [13]. λ_l (liquid thermal conductivity) is calculated from the model proposed by Paradela et al [14] and λ_s (solid thermal conductivity) was estimated to be $0.6 \text{ Wm}^{-1} \text{K}^{-1}$ [9].

Configuration

The conservation equations were solved by using a 2D computational domain that reproduce the annular geometrical configuration of the experiment performed by Veiga et al. [15] (Fig.1), with $L = 1.05 \text{ m}$, $D_{in} = 19 \text{ mm}$, $D_{ex} = 34 \text{ mm}$. The same fluid (19 species), 79.70% $\text{C}_{12}\text{H}_{26}$ and 20.30% parafinas ($\text{C}_{22}\text{H}_{46}$ to $\text{C}_{39}\text{H}_{80}$) was also considered, with $\text{WAT} = 36.5 \text{ }^\circ\text{C}$ (309.65 K).

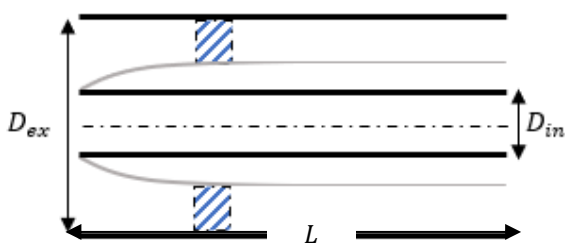


Figure 1 – Domain of interest: annular pipe

Boundary and Initial Conditions

At the inlet, velocity u_{in} and temperature $T_{hot} = 38^\circ\text{C}$ were imposed, as employed in the experiment conducted by Veiga et al. [15], corresponding to an inlet Reynolds number $Re = \rho_{in} u_{in} D_h / \mu_{in} = 743$ ($D_h = D_{ex} - D_{in}$). Further, the same external annular wall temperature equal to T_{hot} was kept constant. Axial diffusion was neglect at the exit. Here, the inner annular wall temperature is varied to create different scenarios.

For all cases, the initial condition correspond to a steady state flow at constant temperature T_{hot} , which is above WAT, therefore, without any deposit.

For each case, different cooling periods (5 min; 10 min; 20 min; 30 min and 60 min) of the inner wall were imposed. After each cooling period, the annular inner wall was heated at a rate of $0.53 \text{ }^\circ\text{C/s}$.

Results and Discussion

Figures 2, 3 and 4 present the fields of solid volumetric fraction, velocity magnitude and temperature at different time instants of the cooling and heating period of the annular inner wall. In order to facilitate the interpretation of the results, the axial axis of the graphs is scaled 1:75. The results presented here refers to a cooling period of 10 minutes, in this case, the inner wall reached $15.6 \text{ }^\circ\text{C}$.

In Figure (2), it is possible to see that after 40s of heating, the wax begins to be removed, and at 100s almost all the wax has been removed from de annular duct. Referring to Fig. (3), one can note that as the inner wall is heated, the deposit detaches from the wall, and starts moving, showing a maximum value of 0.12 m/s . Finally, in Fig. (4) it is interesting to observe that for the evaluated case, the deposit being removed still remains at temperatures below the WAT.

Conclusions

The present study was able to numerically evaluated the heating removal strategy of the wax deposit. Through this study, it was possible to follow the behavior of the wax deposit in relation to the evolution of the velocity and temperature field. The heat removal time required after a certain cooling period was also identified. Finally, the use of the mathematical model based on the mixture model [9] and thermodynamics model [12] are promising methodologies not only regarding the prediction of the wax deposit formation but also to evaluate the removal of the wax deposit by heating.

Acknowledgments

The authors would like to thank to Coordenação de Aperfeiçoamento do Pessoal de Nível Superior – Brasil (CAPES), to Conselho Nacional de Desenvolvimento Científico e Tecnológico – Brasil (CNPq), to Petrobras and to TotalEnergies in Brazil for their support to carry out this present work.

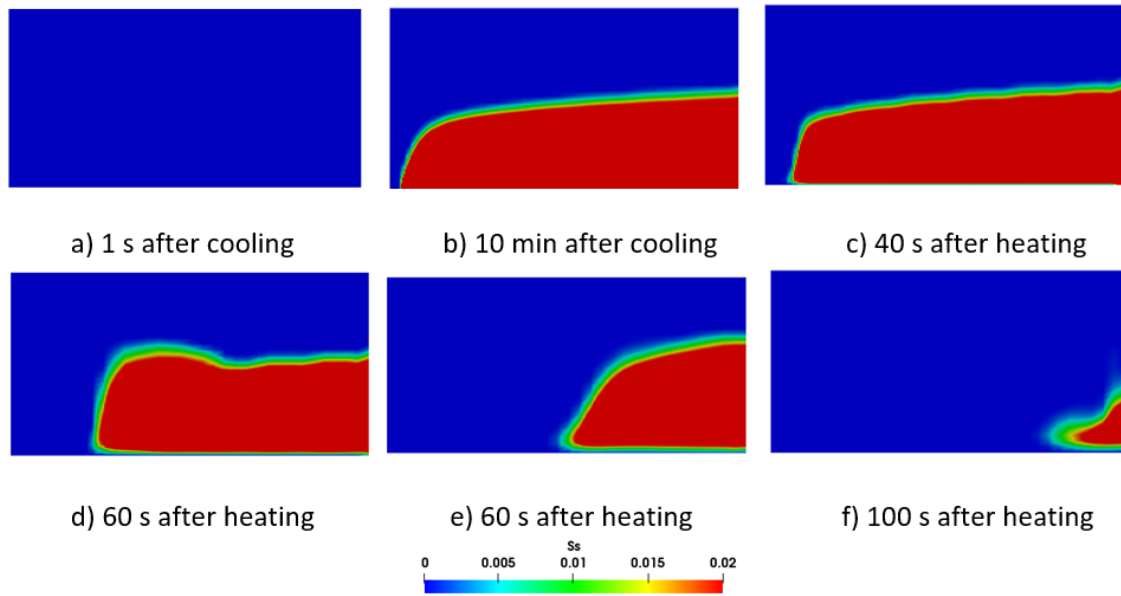


Figure 2. Solid Fraction Field (S_s)

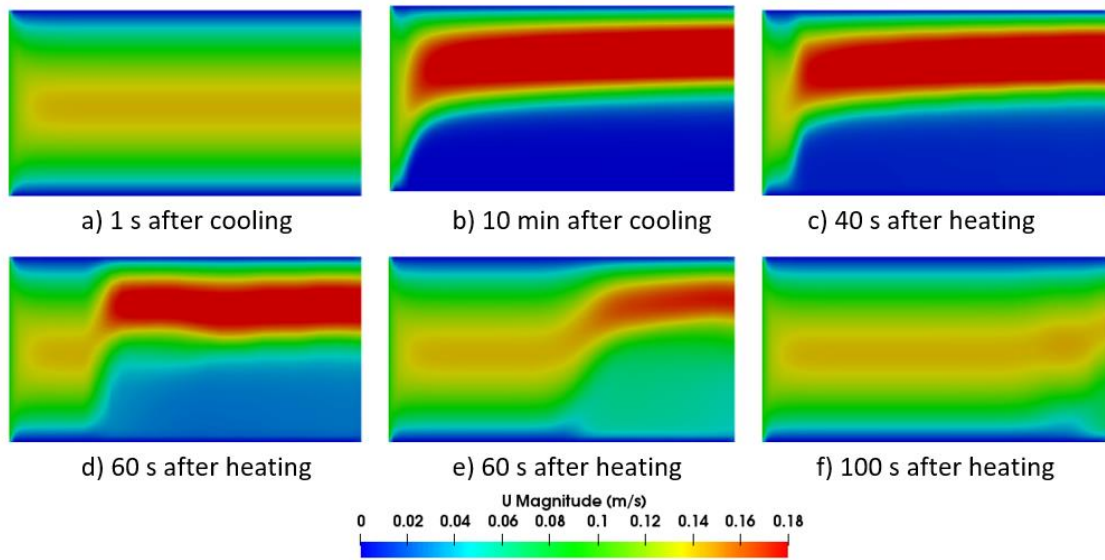


Figure 3. Velocity Magnitude Field

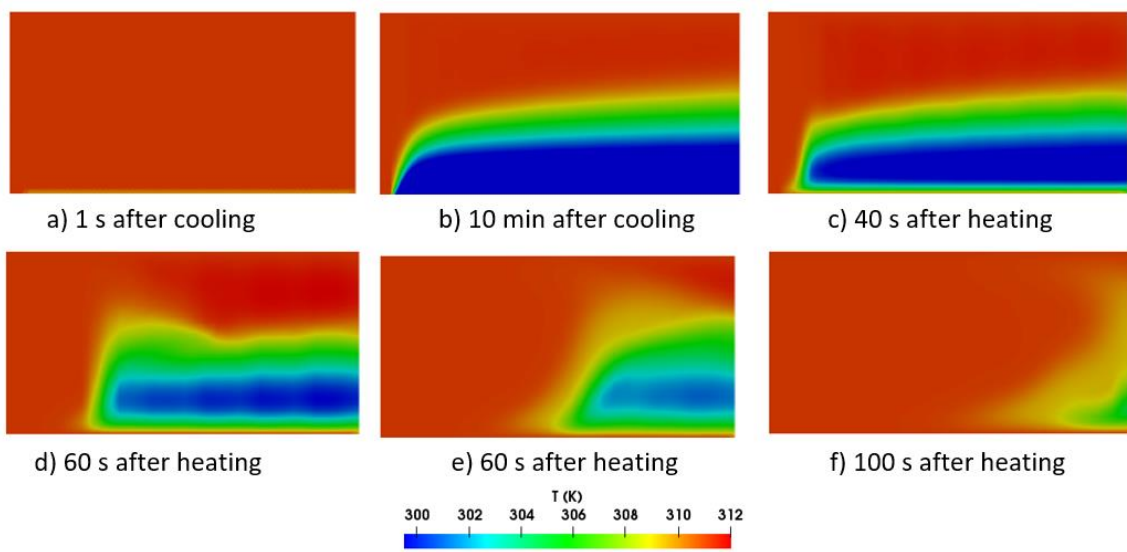


Figure 4. Temperature Field

Responsibility Notice

The authors are the only responsible for the paper content.

References

- [1] Mehrotra, A. K., Ehsani, S., Haj-Shafiei, S., and Kasumu, A. S. A review of heat-transfer mechanism for solid deposition from "waxy" or paraffinic mixtures. *The Canadian Journal of Chemical Engineering*. 98 (12), 2463-2488, 2020.
- [2] Lee, J., Mahir, L. H. A., and Larson, R. G. Experimental Investigation of Time-Dependent Thickness and Composition of Multicomponent Wax Deposits on Cold Surfaces. *Energy & Fuels*. 34 (10), 12330-12339, 2020.
- [3] Wang, W., Huang, Q., Liu, Y., and Sepehrnoori, K. Experimental study on mechanisms of wax removal during pipeline pigging. in *SPE Annual Technical Conference and Exhibition*, OnePetro, 2015.
- [4] Sousa, A., Matos, H., and Guerreiro, L. Preventing and removing wax deposition inside vertical wells: a review. *Journal of Petroleum Exploration and Production Technology*. 9 (3), 2091-2107, 2019.
- [5] Anisuzzaman, S., Krishnaiah, D., and Prathaban, S. N. Comparative Study on Inhibitors Comprising Aromatic and Non-Aromatic Solvents towards Flow Assurance of Crude Oil. *Pertanika Journal of Science & Technology*. 28 (1), 2020.
- [6] Bell, E., Lu, Y., Daraboina, N., and Sarica, C. Experimental Investigation of active heating in removal of wax deposits. *Journal of Petroleum Science and Engineering*. 200, 108346, 2021.
- [7] Veiga, H. M. B., and German, C. Dynamic Operations for Wax Removal, a Challenge on Pre-Salt Oil Wells. in *Offshore Technology Conference*, OnePetro, 2022.
- [8] Ventura, V. F., Mitre, J. F., and Thompson, R. L. A non-isothermal approach to evaluate the impact of the cooling stage on the startup flow of waxy crude oils," *Journal of Non-Newtonian Fluid Mechanics*. 304, 104793, 2022.
- [9] Pereira Fleming, F. Fundamental study of wax deposition under real flow conditions. D.Sc. thesis, Mechaning Eng., PUC-Rio, 2018.
- [10] Holder, G., and Winkler, J. "Wax crystallization from distillate fuels," *J. Inst. Pet*, 51 (499), 228-252, 1965.
- [11] Hayduk, W., and Minhas, B. Correlations for prediction of molecular diffusivities in liquids. *The Canadian Journal of Chemical Engineering*. 60 (2) 295-299, 1982.
- [12] Coutinho, J. A., Mirante, F., and Pauly, J. A new predictive UNIQUAC for modeling of wax formation in hydrocarbon fluids. *Fluid phase equilibria*. 247 (1-2), 8-17, 2006.
- [13] Queimada, A. J., Marrucho, I. M., Coutinho, J. A., and Stenby, E. H. Viscosity and liquid density of asymmetric n-alkane mixtures: measurement and modeling. *International journal of thermophysics*. 26, (1), 47-61, 2005.
- [14] Paradela, F., Queimada, A., Marrucho, I., Neto, C., and Coutinho, J. Modeling the thermal conductivity of pure and mixed heavy n-alkanes suitable for the design of phase change materials. *International journal of thermophysics*. 26 (5), 1461-1475, 2005.
- [15] Veiga, H. M., Boher e Souza, L., Fleming, F. P., Ibanez, I., Linhares, R. C., Nieckele, A. O., and Azevedo, L. F. A. Experimental and Numerical Study of Wax Deposition in a Laboratory-Scale Pipe Section under Well-Controlled Conditions. *Energy & Fuels*, 34 (10), 12182-12203, 2020.